Preprint typeset in JINST style - HYPER VERSION

Optimizing Liquid Scintillators for Low Energy Events via Wavelength-Shifter and Quantum-Dot Doping

R. Schofield*[a], B. Naranjo [a], Y. Ungar[a], C. Coy[a], C. Aberle[a], T. De Guillebon[a], A. Ierokomos[a], L. Winslow[a]

[a] *University of California, Los Angeles, Los Angeles, CA 90095, USA*
E-mail: rschofield@physics.ucla.edu

ABSTRACT: Liquid scintillator-based detectors can be made more sensitive to low energy events by increasing the scintillator's light yield and enabling direction reconstruction of particles. This study presents the optimal concentration of wavelength-shifter 2,5-Diphenyloxazole (PPO) in various solvents. The light yield of seven different scintillators (Toluene, Pseudocumene (PC), Linear Alkyl Benzene (LAB), Phenylcyclohexane (PCH), Phenyl-o-Xylyl Ethane (PXE) and two grades of Di-Isopropyl Napthalene (DIN)) are measured and modeled as a function of the concentration of PPO. In addition, the optical properties of 2 g/L PPO in toluene doped with quantum-dots (QDs) are measured. QDs' ability to fine-tune the absorption and emission spectra of liquid scintillators demonstrate their viability to conserve the directional Cherenkov signal produced by interactions in the liquid scintillator.

*corresponding author

Contents

1. Introduction

The aim of this study is to theorize an ideal liquid scintillator for observing low energy events. This is achieved by maximizing the light yield by choosing the scintillator liquid and the 2,5-Diphenyloxazole (PPO) concentration while maintaining control over the emission and absorption spectrum of a scintillator with quantum-dots (QDs) to preserve the directional information inherent in Cherenkov radiation produced in scintillator interactions.

Table 1. Solvents and solute names or abbreviations used in this paper, the corresponding IUPAC names, CAS numbers and information on the source of the chemicals.

Name	IUPAC Name	CAS Number	Source Information
Toluene	Methylbenzene	108-88-03	Sigma Aldrich [20] (Chromasolv Plus)
Pseudocumene (PC)	1,2,4-Trimethylbenzene	95-63-6	Aldrich (98 %) [20]
Linear Alkyl Benzene (LAB)	various chain lengths	67774-74-7	Cepsa/Petresa [21] PETRELAB® 550-Q
Phenyl-o-Xylylethane (PXE)	1,2-Dimethyl-4-(1-Phenyl-Ethyl)-Benzene	6196-95-8	Dixie Chemical Company [22]
Di-Isopropylnapthalene (DIN)	Isomer mixture	38640-62-9	courtesy of PerkinElmer [23]
Di-Isopropylnapthalene, high purity (DIN HP)	Isomer mixture	38640-62-9	courtesy of PerkinElmer [23]
Phenylcyclohexane (PCH)	Cyclohexylbenzene	827-52-1	Aldrich ($\geq$ 97 %) [20]
Diphenyloxazole (PPO)	2,5-Diphenyloxazole	92-71-7	Aldrich (99 %) [20] suitable for scint.

1.1 Liquid Scintillators

When charged particles propagate through a scintillator, electrons in the π-bonds of the aromatic rings are readily excited [17]. The absorption and emission spectra of a single-molecule based scintillator overlap. In order to prevent degradation of efficiency due to the reabsorption of scintillation light by the scintillator, the liquid scintillator (a solute) was mixed with a wavelength shifter (a solvent). The wavelength shifter absorbs the energy from the excited electron and then releases light of a longer wavelength to which the scintillator is more transparent. Light yield, the number of photons produced per deposited energy, is a vital property of the scintillator because it relates directly to the energy resolution of a scintillator-based detector. Optimizing the energy transfer between solvent and solute molecules maximizes the light yield.

The concentration of the wavelength shifter PPO in each scintillator candidate listed in Table 1 was adjusted and the relative light yields of these binary scintillator mixtures were compared. PPO concentration affects the light yield through two competing mechanisms. The efficiency of energy transfer from solvent to solute increases with increasing PPO concentration. At the studied PPO concentrations, the energy transfers are predominantly non-radiative Förster energy transfers [29, 30], but the emission and re-absorption of real photons or collision energy transfer and others [31] also contribute to the overall effective energy transfer rate. There also is the effect of self-quenching [17] which becomes more important at higher PPO concentrations. In this process, two PPO molecules interact with each other and no light is emitted. The light yield $I(c_{PPO})$ as a

function of PPO concentration c_{PPO} can be described by the equation

$$I(c_{PPO}) = p_1 \cdot \frac{1}{1 + p_2/c_{PPO}} \cdot \frac{1}{1 + p_3 \cdot c_{PPO}} \tag{1.1}$$

where p_1, p_2 and p_3 are three solvent specific parameters: p_1 characterizes the maximum light yield without self-quenching, p_2 the effectiveness of energy transfer from solvent molecules to solute molecules, and $p3$ the effect of self-quenching. For details on the derivation of these types of equations see [32, 33] and references therein.

1.2 Quantum-Dots

Quantum-Dots are semiconducting nanocrystals. The size of a QD is inversely proportional to its band gap and therefore proportional to the wavelength of light it absorbs and emits. Doping scintillator with The wavelength of the absorbed and emitted light can be controlled by doping the scintillator with QDs. QDs can thus be used as a tool to obtain a directional signal from particles (and ultimately to reduce background signals) through the mechanism described below.

Cherenkov radiation is emitted whenever a charged particle travels through a medium at a speed greater than the phase velocity of light in that medium. Unlike scintillation light that is emitted isotropically, Cherenkov light is radiated in a cone that contains the directional information of the incident particle. Cherenkov light is multi-chromatic and has a broad energy distribution. Doping the scintillator with QDs that absorb and emit only high energy photons enables the longer wavelengths of Cherenkov light to travel toward the detector unimpeded by the scintillation process. Because long wavelengths travel faster than short wavelengths of light in a medium due to chromatic dispersion and because the scintillation absorption and emission process takes time, the long wavelengths of Cherenkov light will reach the detector before the scintillation light, enabling measurement of Cherenkov light and ultimately directional reconstruction of particle trajectory. Furthermore, adding QDs to the scintillator solvent generally narrows the absorption spectrum of the liquid scintillator. Narrowing the absorption spectrum of the scintillator is important because for low energy events, there are very few long-wavelength photons emitted. For example, a 1 MeV electron emits only 83 Cherenkov photons between 370-550 nm[18].

Unfortunately, doping liquid scintillators with QDs comes at the cost of lower light yields as shown in Section 3.1.3 and discussed Section 3.2.2. Fortunately, this can be partially countered by choosing the emission peak to match the optimal wavelength for the quantum efficiency of the photomultiplier tube (PMT)[34]. The QDs of various emission and absorption spectra that undergo study for suitability are listed in Table 2.

2. Experimental

The light yield of candidate liquid scintillators with varying amounts of PPO and different QDs was measured by collecting the charge produced by a gamma ray irradiated scintillator with a PMT. In addition, the emission and absorption spectrum of the QDs were measured with two different spectrophotometers. The details of the experimental setup are explained below followed by a description of the sample handling.

Table 2. Quantum-Dot composition and source information.

Composition (core/shell)	Source Information
CdS	NN-Labs-CS360[24]
CdS	NN-Labs-CS400[24]
CdS	MKN-CdS-T360[25]
CdS	MKN-CdS-T380[25]
CdS	MKN-CdS-T400[25]
CdS/ZnS	Ocean NanoTech QZR-400-0010[26]
CdS/ZnS	Ocean NanoTech QZR-425-0010 [26]
CdSeS/ZnS	Crystalplex NC-450-A [27]

2.1 Light Yield Setup

2.1.1 Setup

The setup is illustrated in Figure 1. A (1 cm×1 cm×3.5 cm) UV-transparent quartz cell (Starna 21-Q-10 [28]) holds the scintillator mixtures. The cell is coupled to the PMT with transparent silicone optical grease (Saint Gobain BC-630) with a similar index of refraction to the cell and PMT glass so that light losses due to reflection are minimized. The quartz cell is then secured in a reflective white Teflon block to further increase the light collection efficiency. The scintillator is excited by a ^{137}Cs source with an activity of $\approx$1 μCi (=37 kBq). The source is attached to the outside of the Teflon block. Isotope ^{137}Cs undergoes beta decay with the subsequent emission of a single 662 keV gamma. The emitted gamma rays enter the quartz cell, then typically Compton scatter with electrons, which excite the scintillator. Cherenkov light is also produced from electrons with energies above a given threshold as discussed in Section 1.2 . A fraction of the emitted optical photons hit the photocathode of a Hamamatsu R1828-01 PMT [34]. A Hamamatsu E2979-500 base [35] is used, and the high voltage of -1675 V is provided by a LeCroy 1454 high voltage system. The charge incident on the photocathode produce pulses which are recorded by an AlazarTech ATS9870 PCI waveform digitizer [36].

2.1.2 Photomultiplier Tube Calibration

2.1.3 Sample Handling and Procedure

In order to ensure reproducible and accurate measurements, a sample handling procedure is defined. In particular, contamination of the samples with dust, residual chemicals and oxygen is avoided.

The bottles that store the samples are rinsed with isopropanol, cyclohexane, dried and finally rinsed with the solvent. In addition, the bottles are sealed under N_2 to reduce the amount of oxygen in contact with the sample. Oxygen interferes with the light production processes (oxygen quench-

ing [17]) and leads to a loss of light output. The lids of the bottles are sealed with Teflon tape and electric tape to further limit the amount of oxygen entering the bottle.

The quartz cell is also cleaned thoroughly when samples are changed. The optical grease on the outside is removed with ethanol and on the inside it is washed with isopropanol then dried with N_2 twice, washed with cyclohexane, and again dried with N_2. The amount of liquid scintillator sample in the cell is kept constant to avoid effects due to differences in light collection. Before each measurement, a pipet is inserted into the liquid to slowly purge the samples with nitrogen for about 10 minutes to actively remove remaining oxygen.

The coupling of the cell to the PMT is done consistently, and the PMT is aligned in the same way in order to avoid effects due to the earth's magnetic field. Section 3.1 presents the studies that determine measurement reproducibility. The quartz cell containing the liquid scintillator sample is placed in the dark box setup as described in the previous section, and a measurement is performed for a duration of 30 minutes.

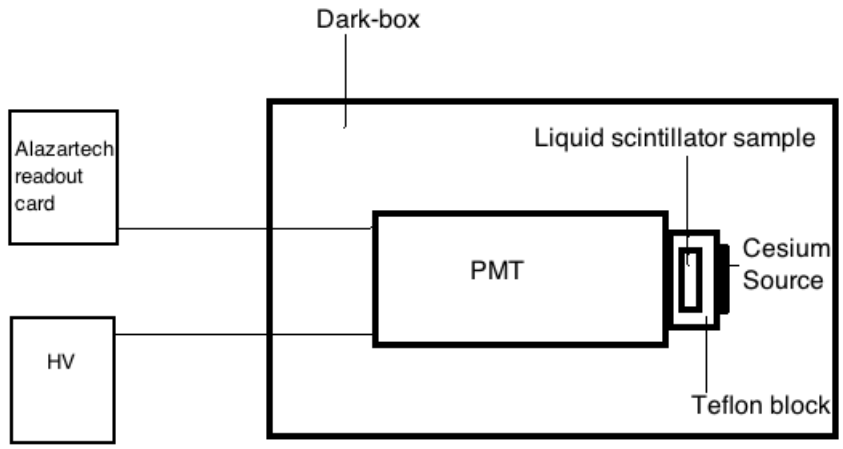

Figure 1. Schematic view of the light yield measurement setup.

2.2 Absorption and Emission Setup

2.2.1 Setup

A Perkin Elmer Lambda 25 UV/Vis is used for measuring the emission spectrum and a Shimadzu UV3101 for measuring absorption spectrum of the QD doped liquid scintillators. Both instruments

utilize a double-beam setup. White light from deuterium UV lamp and a halogen lamp produce the beams. [**?**]

2.2.2 Sample Handling and Procedure

To measure the absorption spectrum of each quantum-dot sample, the following procedure is executed. A (1 cm$\times$1 cm$\times$3.5 cm) UV-transparent quartz cell (Starna 21-Q-10 [28]) is rinsed with toluene to dissolve any residue on the wall. Next, the cell is soaked in hydrochloric acid for 5 minutes to clean the cell and destroy any remaining QD. To wash away the hydrochloric acid and the residue QD constituents, the quartz cell is rinsed with distilled water and is then subjected to three iterations of liquid isopropyl alcohol evaporated by nitrogen gas. Since all of the QD samples are dissolved in toluene, a background absorption spectrum analysis is required to isolate the quantum-dot spectrum. A background scan is performed with a vial filled with pure toluene. The toluene is then replaced with the QD sample, and the absorption scan is performed.

The cleaning procedure for the emission spectrum measurements is the same as the procedure for the absorption trials. The emission spectrum is measured by a Perkin Elmer Lambda 25 UV/Vis and does not require a background toluene scan.

3. Results

This section presents the analysis methodology as well as the main results, namely the light yield measurements as a function of PPO concentrations for each of the solvents listed in Table 1 and for the different QDs listed in Table 2 dissolved in toluene with 2 g/L of PPO added. The emission and absorption spectrum of the QD scintillators are also measured.

3.1 Light Yield

3.1.1 Signal Analysis

- Baseline: At the beginning of each waveform, 100 samples are averaged to get the baseline value.
- Pulse finder: Pulses are defined as a consecutive series of samples below the rounded baseline value.
- Pulse times: For each pulse the start time is defined as the time where the waveform falls below the rounded baseline value. The stop time is set once the pulse reaches this value again.
- Charge: The integral of the baseline-subtracted waveform between the start and stop times.

The duration of each run is around thirty minutes and during this time on the order of $3 \cdot 10^5$ waveforms are recorded. Each pulse corresponds to one gamma ray interaction within the liquid scintillator. The amount of light collected by the PMT is dependent on the scattering angle of the electron that is produced by Compton scattering of the 0.662 MeV gamma ray. The result of the charge calculation is placed in a histogram, Figure 3. Since the Compton effect is the dominant mechanism, this histogram is a Compton spectrum. The events where the Compton

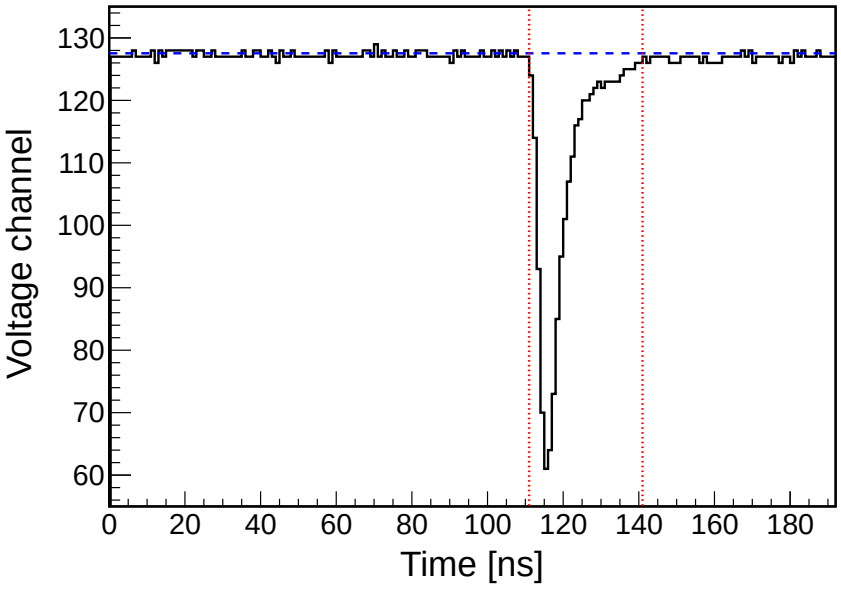

Figure 2. Example waveform recorded by the AlazarTech digitizer card. For each waveform, 192 samples are taken with a rate of 1Gs/s. The blue, dashed line is the baseline which is calculated for each waveform. The red, dotted lines show the start and stop time for the main pulse in this waveform. Integration of the baseline subtracted waveform between start and stop yields 520. The trigger threshold is set at voltage channel 116.

scattered electron obtained close to the maximal energy, 478 keV for the 662 keV gammas from ^{137}Cs, is associated with events at the right end of this spectrum. Multiple pulses are found for each waveform, including baseline fluctuations. The small fake pulses from baseline fluctuations did not affect analysis. In order to compare different scintillator mixtures, the charge where the number of events dropped to half of the Compton edge maximum is compared, Figure 3. This quantity is proportional to the scintillator light yield. For practical reasons and because this study only looks at relative light yield, results are presented in arbitrary charge units instead of real charge units.

3.1.2 Investigation of Uncertainties

This section focuses on the reproducibility of a measurement and estimates the error of a single measurement based on the sample handle procedure defined in Section 2.1.

The error due to differences in the procedure of coupling the scintillator cell to the PMT glass is measured. For this test, the same sample, LAB with 5 g/L PPO, is sealed in the cell and only the coupling is renewed. The RMS divided by the sample mean for several trials is 0.30 %. This number is used as a rough estimate for the relative error of a single measurement due to differences in the coupling. The small uncertainty in the determination of the charge value from the histograms, Figure 3, is already included here. The relative spread of 0.30 % is negligible compared to other uncertainties discussed below.

The effect of oxygen is also studied quantitatively. A comparatively 24-day old sample of DIN HP with 5 g/L PPO is purged with nitrogen bubbles for 10 minutes as in the standard measurement

procedure and is measured. Then the sample is opened and left in contact with oxygen for 15 minutes. It is then re-measured without nitrogen purging. The charge value dropped by 2.04 %. After an additional 3 hours of contact with oxygen the same is measured. The relative difference between the first and the last measurement is about 6.92 %, indicating the importance of nitrogen purging and reproducible procedures in preventing oxygen from entering the scintillator.

In order to estimate the total error of a single light yield measurement, the same sample with the full sample change protocol, as described in Section 2.1, is measured repeatedly. For these measurements an older sample, 7 weeks after mixing, of DIN HP is used as well as a standard DIN sample, 3-4 weeks old. For the older samples, 10 minutes of nitrogen purging is not sufficient to remove oxygen. The effect of differences in the oxygen removal is included in these reproducibility measurements. However, it is difficult to assess exactly how oxygen contamination affects the measurements when the full measurement protocol is applied. The RMS for these data sets is is about 3.70 % and is regarded as a rough estimate of the relative uncertainty of a single light yield measurement.

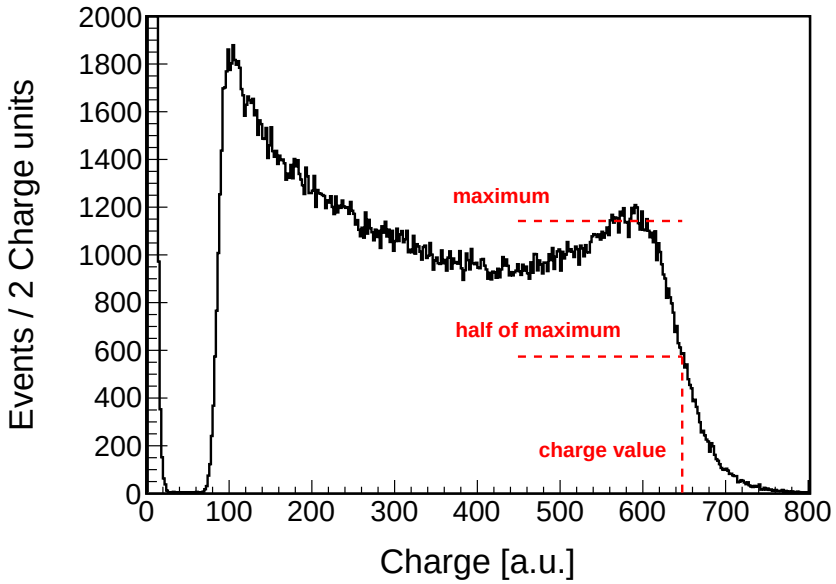

Figure 3. Example charge spectrum. To compare different scintillators, the charge at a characteristic point close to the true Compton edge is determined.

3.1.3 Light Yield Results

Table 3 contains the light yield results for the different liquid scintillator candidates described in Table 1.

In Figure 3, each plot shows the solvent's characteristic charge at the Compton edge as a function of PPO concentration in g/L. Concentrations of 0.5 g/L, 1 g/L, 2 g/L, 5 g/L, 10 g/L and 50 g/L have been used. Tables 4 and 5 include the fit results; the parameters p1, p2 and p3 describe the light yield normalization, the energy transfer from solvent to solute and the self-quenching effect, respectively.

Table 3. Listed below are the fit results for each solvent's data set. The fit parameters and their errors are given and their respective χ^2 values, and the probabilities to get a worse χ^2 than the observed one. Since we have 6 data points and 3 parameters in the fit the number of degrees of freedom is 3.

Solvent	p_1 [a.u.]	p_2 [g/L]	p_3 [g/L]	χ^2	prob. %	max. LY
Toluene	681 ± 10	0.09 ± 0.014	0.019 ± 0.001	0.55	91	627 (at 2.2 g/L)
PC	578 ± 47	2.09 ± 0.37	0.014 ± 0.004	5.30	15	422 (at 12.2 g/L)
LAB	525 ± 24	0.36 ± 0.01	0.013 ± 0.003	4.33	23	462 (at 5.3 g/L)
PXE	694 ± 25	0.48 ± 0.96	0.013 ± 0.002	2.55	47	596 (at 6.1 g/L)
DIN	668 ± 19	0.27 ± 0.01	0.007 ± 0.001	2.34	50	613 (at 6.2 g/L)
DIN HP	673 ± 40	0.19 ± 0.08	0.005 ± 0.003	10.6	1	631 (at 6.1 g/L)
PCH	634 ± 29	0.34 ± 0.07	0.012 ± 0.003	6.11	11	562 (at 5.4 g/L)

As clearly stated in Table 5, toluene produces the highest light yield around 2.2 g/L. QD scintillators are doped with 2 g/L PPO for comparison with 2 g/L PPO in toluene. The light yield as a function of QD emission wavelength is plotted in Figure 6.

3.2 Emission and Aborption Spectrum of Quantum-Dot Doped Liquid Scintillators

3.2.1 Signal Analysis

Various trials are conducted to test the output signal of both the Perkin Elmer Lambda 25 UV/Vis and the Shimadzu UV3101 spectrophotometers[19]. The error is described by the following equation: 3.1.

$$A(x) = \log_{10}\left(\frac{I(x)}{I(0)}\right) \tag{3.1}$$

where $I(0)$ is the intensity of the beam before transiting the quartz cell and $I(x)$ is the intensity after it passes through the cell.

The errors for the Perkin and Shimadzu spectrophotometers are $A = \pm 0.00075$ and $A = \pm 0.002$ respectfully. These errors are in close agreement with the manufactures specifications[**?**].

3.2.2 Absorption and Emission Results

The absorption and emission spectrum of the QDs were extensively probed, and the results are graphed in Figures 7 and 8 respectfully. As stated in Section 1.2 and proved in 3.1.3, the light yield of the QD doped scintillators is much lower than that of the binary mixture of toluene with PPO. This is due to the overlap in emission and absorption QD spectrum coupled with low quantum efficiency [18]. (I'm creating a figure that shows the overlap for emission and absorption for each quantum dot). The absorption spectrum of the QD doped liquid scintillators are narrower than that of toluene doped with 2 g/L PPO. (How can we back this? Need to take an absorption and emission scan of toluene + 2g/L PPO.)

4. Conclusion

Detection of low energy events in liquid scintillators require high light yield and preservation of Cherenkov radiation. This study successfully measures and models the light yield of seven scintillator liquids as a function of wavelength-shifter concentration in order to find the maximum light yield of each candidate. Furthermore, an extensive study on the effects of quantum-dot doping of toluene with 2 g/L of PPO in solution are analyzed. QDs reduce the width and control the location of the absorption spectrum peak. This allows the quantum efficiency of the photocathode to be matched and minimized the amount of Cherenkov radiation absorbed by the liquid scintillator.

Regrettably, QDs significantly reduce the light yield of scintillators. With improved technology in quantum dot production, QDs with better characteristics such as shorter emission wavelengths are expected to become available in the near future. These QDs should be able to improve the light yield of quantum dot-doped scintillator.

References

[1] E. Majorana, *Teoria simmetrica dell'elettrone e del positrone*, *Il Nuovo Cimento* **14** (1937) 171.

[2] W.H. Furry, *On Transition Probabilities In Double Beta-Disintegration*, *Phys. Rev.* **56** (1939) 1184.

[3] K. Zuber, *Neutrino Physics*, Taylor and Francis Group, 2004.

[4] V.I. Tretyak, Y.G. Zdesenko, *Tables of double beta decay data*, *Atomic Data and Nuclear Data Tables* **61** (1995) 43.

[5] S.R. Elliott and P. Vogel, *Double Beta Decay*, *Annu. Rev. Nucl. Part. S.* **52** (2002) 115.

[6] A. Barabash, *Double beta decay experiments*, Phys. Part. Nucl. **42** (2011) 613 [arXiv:1107.5663].

[7] B. Schwingenheuer, *Status and prospects of searches for neutrinoless double beta decay*, *Ann. Phys.* **525** (2013) 269.

[8] O. Cremonesi and M. Pavan, *Challenges in Double Beta Decay*, arXiv:1310.4692.

[9] J. Schechter and J.W.F. Valle, *Neutrinoless double-β decay in SU(2)$\times$U(1) theories*, *Phys. Rev. D* **25** (1982) 2951.

[10] H.V. Klapdor-Kleingrothaus, I.V. Krivosheina, A. Dietz and O. Chkvorets, *Search for neutrinoless double beta decay with enriched 76Ge in Gran Sasso 1990-2003*, *Phys. Lett. B* **586** (2004) 198.

[11] H.V. Klapdor-Kleingrothaus and I. Krivosheina, *The evidence for the observation of $0\nu\beta\beta$ decay: the identification of $0\nu\beta\beta$ events from the full spectra*, *Mod. Phys. Lett. A* **21** (2006) 1547 (2006).

[12] H.V. Klapdor-Kleingrothaus et al. (Heidelberg-Moscow Collaboration), *Latest results from the HEIDELBERG-MOSCOW double beta decay experiment*, *Eur. Phys. J. A* **12** (2001) 147.

[13] M. Agostini et al. (GERDA collaboration), *Results on Neutrinoless Double-β Decay of ^{76}Ge from Phase I of the GERDA Experiment*, *Phys. Rev. Lett.* **111** (2013) 122503.

[14] A. Gando et al. (KamLAND-Zen Collaboration), *Limit on Neutrinoless $\beta\beta$ Decay of ^{136}Xe from the First Phase of KamLAND-Zen and Comparison with the Positive Claim in ^{76}Ge*, *Phys. Rev. Lett.* **110** (2013) 062502.

[15] C. Kraus, S.J.M. Peeters, *The rich neutrino programme of the SNO+ experiment*, *Prog. Part. Nucl. Phys.* **64** (2010) 273.

[16] J. Hartnell for the SNO+ collaboration, *Neutrinoless Double Beta Decay with SNO+*, *J. Phys. Conf. Ser.* **375** (2012) 042015.

[17] J.B. Birks, *The Theory and Practice of Scintillation Counting*, Pergamon Press, 1964.

[18] C. Aberle, J.J. Li, S. Weiss and L. Winslow, *Measuring directionality in double-beta decay and neutrino interactions with kiloton-scale scintillation detectors* , 2014 *JINST* **9** P06012.

[19] C. Aberle, J.J. Li, S. Weiss and L. Winslow, *Optical properties of quantum-dot-doped liquid scintillators*, 2013 *JINST* **8** P10015.

[20] http://www.sigmaaldrich.com (2014).

[21] http://www.cepsa.com (2014).

[22] http://www.dixiechemical.com (2014).

[23] http://www.perkinelmer.com (2014).

[24] http://www.nn-labs.com (2014).

[25] http://mknano.com (2014).

[26] http://www.oceannanotech.com (2014).

[27] http://www.crystalplex.com (2014).

[28] http://www.starnacells.com (2014).

[29] T. Förster, *Zwischenmolekulare Energiewanderung und Fluoreszenz*, *Ann. Phys.* **2** (1948) 55.

[30] T. Förster, *Transfer Mechanisms of electronic excitation*, *Discuss. Faraday Soc.* **27** (1959) 7.

[31] D.L. Dexter, *A theory of sensitized luminescence in solids*, *J. Chem. Phys.* **21** (1953) 836.

[32] C. Buck, F.X. Hartmann, D. Motta, S. Schönert, *Energy transfer and light yield properties of a new highly loaded indium(III) β-diketonate organic scintillator system*, *Chem. Phys. Lett.* **435** (2007) 252.

[33] C. Aberle, C. Buck, F.X. Hartmann and S. Schönert, *Light yield and energy transfer in a new Gd-loaded liquid scintillator*, *Chem. Phys. Lett.* **516** (2011) 257.

[34] Hamamatsu Photonics K.K., *Photomultiplier Tubes R1828-01, R2059* (data sheet), accessed March, 2014: http://www.hamamatsu.com/resources/pdf/etd/R1828-01_R2059_TPMH1259E04.pdf.

[35] Hamamatsu Photonics K.K., *D-Type Socket Assemblies* (data sheet), accessed March, 2014: http://www.hamamatsu.com/resources/pdf/etd/PMT_92-103_e.pdf.

[36] http://www.alazartech.com (2014).

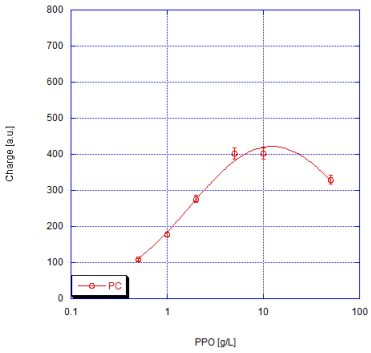

(a) PC

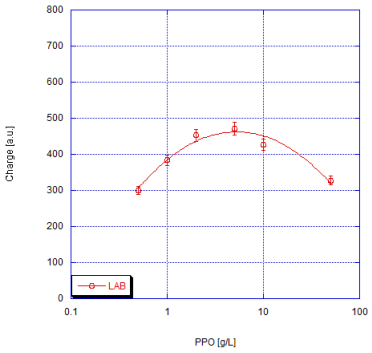

(b) LAB

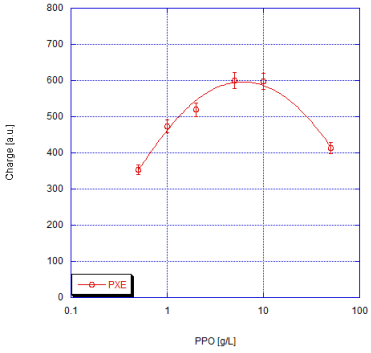

(c) PXE

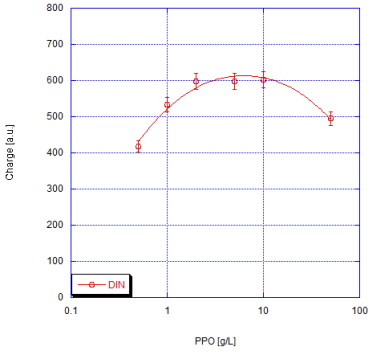

(d) DIN

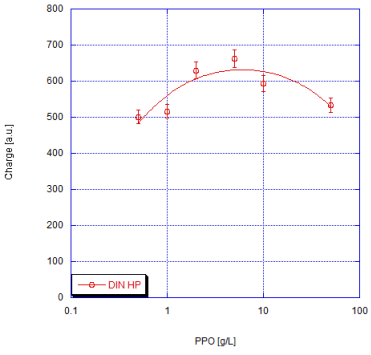

(e) DIN HP

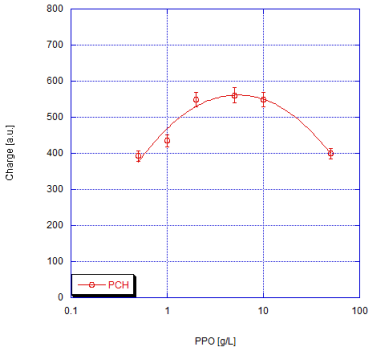

(f) PCH

Figure 4. Show the charge value at the Compton edge (proportional to the light yield) for each of the 6 concentrations of PPO for six of the liquid scintillator candidates. A relative error of 3.7 % was used for each measurement. The red lines show the fit of equation 1.1. Note that the x-axis is logarithmic; the PPO concentrations span two orders of magnitude.

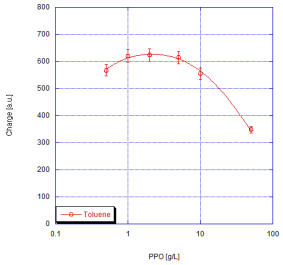

(a) Toluene

Figure 5. Show the charge value at the Compton edge (proportional to the light yield) for each of the 6 concentrations of PPO for toluene. A relative error of 3.7 % was used for each measurement. The red lines show the fit of equation 1.1. Note that the x-axis is logarithmic; the PPO concentrations span two orders of magnitude.

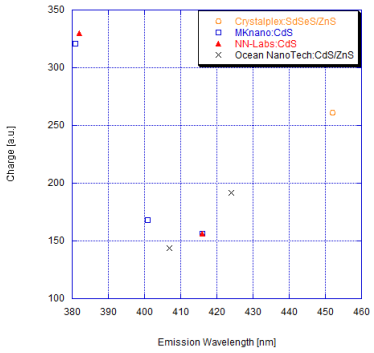

Figure 6. The light yield of quantum-dot doped toluene scintillators with 2 g/L of PPO versus emission wavelength of the QDs.

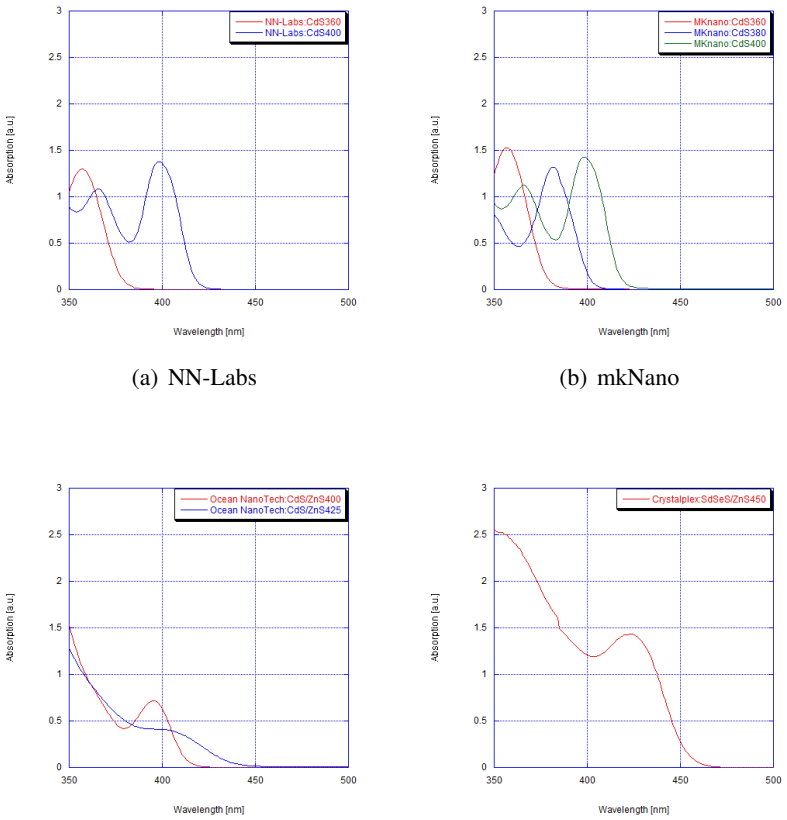

(a) NN-Labs (b) mkNano

(c) Ocean NanoTech (d) Crystalplex

Figure 7. Absorption spectrum of the quantum-dots listed in Table 2 dissolved in toluene and grouped by manufacturer.

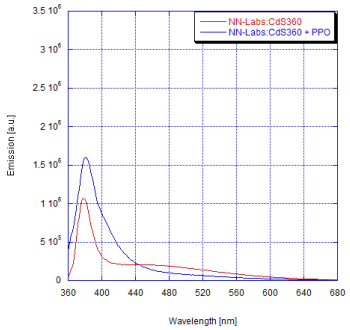

(a)

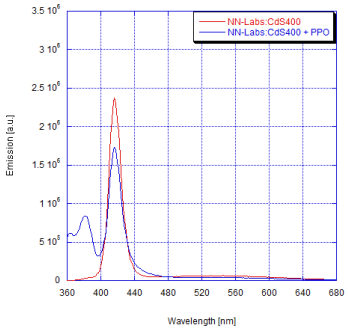

(b)

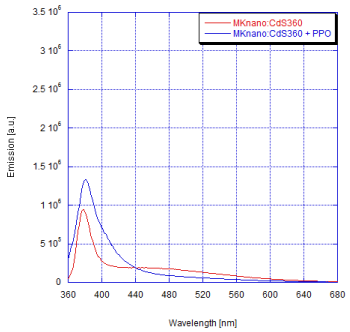

(c)

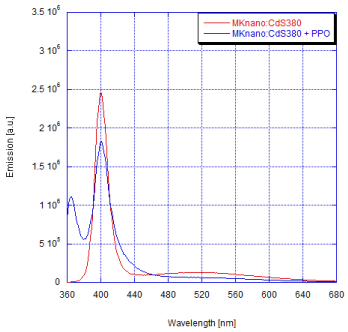

(d)

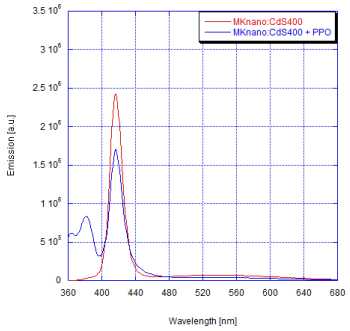

(e)

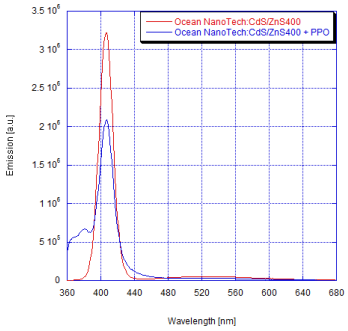

(f)

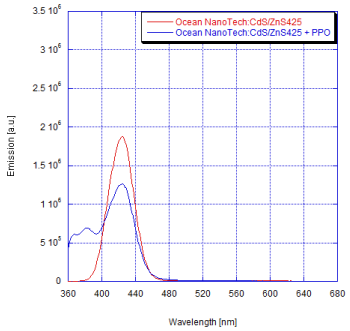

(g)

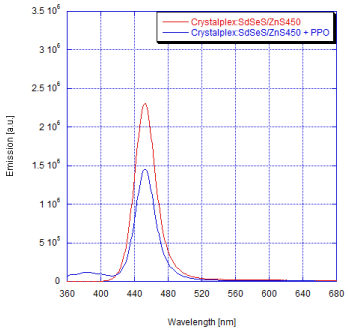

(h)

Figure 8. Emission spectrum of the quantum-dots listed in Table 2 dissolved in toluene with and without 2 g/L of PPO added.